

RSC Advances



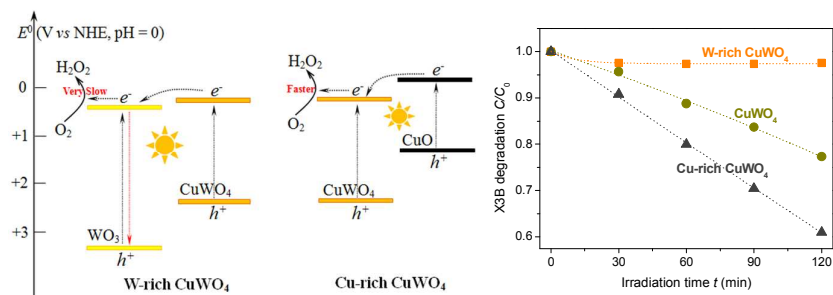
This is an *Accepted Manuscript*, which has been through the Royal Society of Chemistry peer review process and has been accepted for publication.

Accepted Manuscripts are published online shortly after acceptance, before technical editing, formatting and proof reading. Using this free service, authors can make their results available to the community, in citable form, before we publish the edited article. This *Accepted Manuscript* will be replaced by the edited, formatted and paginated article as soon as this is available.

You can find more information about *Accepted Manuscripts* in the [Information for Authors](#).

Please note that technical editing may introduce minor changes to the text and/or graphics, which may alter content. The journal's standard [Terms & Conditions](#) and the [Ethical guidelines](#) still apply. In no event shall the Royal Society of Chemistry be held responsible for any errors or omissions in this *Accepted Manuscript* or any consequences arising from the use of any information it contains.

Graphical abstract:



Cu-rich CuWO₄ prepared at pH 8.5 and 600 °C was more active than other samples for organic degradation under visible light.

Cite this: DOI: 10.1039/c0xx00000x

www.rsc.org/xxxxxx

PAPER

Photocatalytic organic degradation over W-rich and Cu-rich CuWO_4 under UV and visible light

Haihang Chen, and Yiming Xu*

Received (in XXX, XXX) Xth XXXXXXXXX 20XX, Accepted Xth XXXXXXXXX 20XX

DOI: 10.1039/b000000x

Hydrothermal reaction between $\text{Cu}(\text{NO}_3)_2$ and Na_2WO_4 at 170 °C, followed by sintering at 500 °C, resulted in the formation of stoichiometric CuWO_4 at pH 5.2, while the reactions below and above pH 5.2 gave a mixture of CuWO_4 with WO_3 and CuO , respectively. For organic degradation in water under visible light, W-rich and Cu-rich samples were less and more active than CuWO_4 , respectively. A maximum activity was observed with the sample prepared at pH 8.5. Furthermore, this Cu-rich sample shown an activity greatly changing with its sintering temperature, and reaching a maximum at 600 °C. A possible mechanism responsible for the observed activity difference among the samples is proposed, involving the interfacial charge transfer between CuWO_4 and WO_3 or CuO .

Introduction

Heterogeneous photocatalysis for environmental remediation has been studied for many years.^{1–3} Among various semiconductors, TiO_2 has been widely studied, due to its low cost and high activity. However, TiO_2 is active only in UV light, which would limit utilization of solar energy. Recently, CuWO_4 as a visible-light-driven photocatalyst has been received an increasing attention. This semiconductor can absorb light at wavelengths shorter than 540 nm.⁴ Under stimulated solar illumination, the CuWO_4 films, fabricated by spin-coating, reactive cosputtering, spray pyrolysis and electrodeposition, can be used as the photoanodes for water oxidation to O_2 at an applied potential bias.^{5–10} In addition, CuWO_4 powders prepared by a co-precipitation method are also active for organic degradation in aerated aqueous solution under visible light.^{11–13} However, the observed photocatalytic activity of CuWO_4 for organic degradation in water is very low, mainly due to fast recombination of the photogenerated charge carriers. In general, the photocatalytic activity of a semiconductor can be improved by increasing its crystallinity and surface area, and/or through surface modification with suitable co-catalysts. We have recently shown that deposition of CuWO_4 with 1.8 wt % of CuO can increase the activity by 9 times under UV light, and 5 times under visible light for phenol degradation in water.¹³

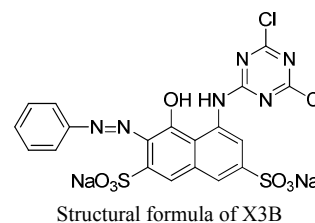
In this article, we report on the hydrothermal synthesis of CuWO_4 , whose chemical composition, crystalline structure and photocatalytic activity are greatly influenced by the solution pH and sintering temperature used for the solid synthesis. Samples were prepared in aqueous solution at 170 °C with $\text{Cu}(\text{NO}_3)_2$ and Na_2WO_4 as precursors. Solids were characterized with several routine techniques, and their photocatalytic activities for organic degradation in water were measured under either UV or visible light. Furthermore, a possible mechanism responsible for the

observed activity difference among the samples is discussed.

Experimental Section

Reagents

Tungstate (VI) sodium dihydrate was purchased from Sinopharm Chemical Reagent Co., Ltd., and a textile azo-dye X3B (Reactive Orange 86) from Jining dye manufacture of China ($pK_a = 4.5$). Copper (II) nitrate trihydrate, phenol and other chemicals in analytical grade were purchased from Shanghai Chemicals Inc., China, and used as received without further purification. The solution pH was adjusted with a dilute solution of NaOH or HCl . Milli-Q water was used throughout this work.



Synthesis

Typically, the aqueous solutions of 0.10 M $\text{Na}_2\text{WO}_4 \cdot 2\text{H}_2\text{O}$ and 0.10 M $\text{Cu}(\text{NO}_3)_2 \cdot 3\text{H}_2\text{O}$ were first prepared. Then the former was added dropwise to the latter under magnetic stirring, followed by pH adjustment to a given value. After further stirring for 30min, and sonication for 30 min, the suspension was transferred into a stainless autoclave, and heated at 170 °C for 20 h. After the reactor cooled down, the particles was collected by centrifuge, thoroughly washed with water, and dried at 60 °C overnight. Finally, the solid was sintered in air at a given temperature for 3 h.

Characterization

X-ray powder diffraction (XRD) pattern was recorded on a D/max-2550/PC diffractometer (Rigaku). According to the (100) diffraction, the crystal size of CuWO_4 was calculated by using Scherrer equation. Adsorption isotherm of N_2 on solid was measured at 77 K on a Micromeritics ASAP2020 apparatus, from which the Brunauer–Emmett–Teller (BET) surface area (S_{BET}) and cumulative pore volume (V_p) were calculated. Scanning electron microscope (SEM) image was recorded on a Hitachi S-4800, attached with EDS (energy-dispersive X-ray spectroscopy). X-ray photoelectron spectroscopy (XPS) data were measured with Kratos AXIS Ultra DLD spectrometer, and calibrated with C1s at 284.8 eV. Diffuse reflectance spectra were recorded on a Shimadzu UV-2550 with BaSO_4 as a reference. The reflectance (R) is transformed to the Kubelka–Munk unit, $F(R) = (1 - R)^2/2R$.

15 Photocatalysis

Reactions were carried out in a Pyrex-glass reactor, thermostated at 25 °C through a recycle system. Light sources were a 300W high pressure mercury lamp (Shanghai Mengya) for UV light, and a 150 W Xenon lamp (USHIO) equipped with a 420 nm cut-off filter for visible light. The light intensity reaching the external surface of the reactor was 1.41, and 5.50 mW/cm^2 for Hg and Xe lamps, respectively, measured with an irradiance meter (Beijing Normal University, China). The suspension (50 mL) containing 1.7 g/L catalyst and 0.066 mM X3B or 0.22 mM phenol was first stirred in the dark for 12 h, and then irradiated with UV or visible light. At given intervals, small aliquots were withdrawn, and filtered through a membrane. Dye concentration was analyzed at 533 nm on an Agilent 8451 spectrometer. Phenol concentration was measured with high performance liquid chromatography on a Dionex Ultimate 3000, equipped with Apollo C18 reverse column, and with 50% CH_3OH aqueous solution as an eluent.

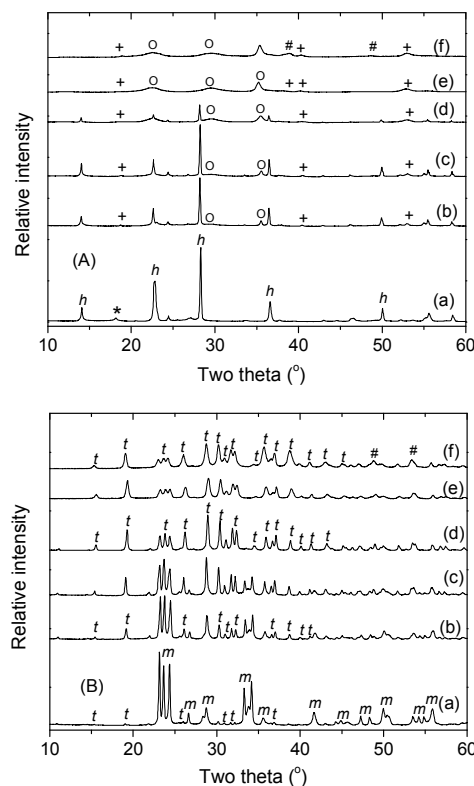
Results and Discussion

Effect of Synthesis pH

The solids were prepared from the reaction between $\text{Cu}(\text{NO}_3)_2$ and Na_2WO_4 in aqueous solution at a fixed temperature (170 °C), but at different pHs (1.1–11.6). Because of that, the samples were different not only in the chemical composition, but also in the crystal structures and optical properties. Element analysis by EDS showed that the mole ratio of Cu to W increased with the solution pH, the value of which was 0.05, 0.24, 0.25, 1.04, 1.86 and 3.00 for the samples prepared at pH 1.1, 2.4, 3.9, 5.2, 8.5 and 11.6, respectively. The relevant EDS spectra of the samples were showed in Fig. S1 (ESI). These results indicate that only the CuWO_4 sample prepared at pH 5.2 was stoichiometric. Below and above this pH, the samples were W-rich and Cu-rich CuWO_4 , respectively. It is highly possible that the W-rich and Cu-rich sample are a mixture of CuWO_4 with WO_3 and CuO , respectively.

In order to confirm this hypothesis, the crystalline phase of the sample was analyzed by XRD. Fig. 1A shows the XRD patterns of the as-prepared samples. The solid obtained at pH 1.1 exhibited series of diffraction peaks mainly due to hexagonal WO_3 (PDF # 33-1387), and partially due to orthorhombic $\text{WO}_3 \cdot 0.33\text{H}_2\text{O}$ (PDF # 35-0270). When the solid was prepared at pH 5.2, the peak intensities of WO_3 and $\text{WO}_3 \cdot 0.33\text{H}_2\text{O}$ were greatly reduced, together with the formation of new crystalline phases of $\text{CuWO}_4 \cdot 2\text{H}_2\text{O}$ (PDF # 33-0503), and $\text{Cu}_2\text{WO}_4(\text{OH})_2$

(PDF# 34-1297).



60 **Fig. 1** XRD patterns of (A) the as-prepared solids at initial pHs of (a) 1.1, (b) 2.4, (c) 3.9, (d) 5.2, (e) 8.5, and (f) 11.6, and (B) the corresponding solids sintered at 500 °C. Note that h = hexagonal WO_3 , m = monoclinic WO_3 , t = triclinic CuWO_4 , (*) = $\text{WO}_3 \cdot 0.33\text{H}_2\text{O}$, (o) = $\text{CuWO}_4 \cdot 2\text{H}_2\text{O}$, (+) = tetragonal $\text{Cu}_2\text{WO}_4(\text{OH})_2$, and (#) = monoclinic CuO .

65 When the synthesis pH was further increased to 11.6, additional peaks at $2\theta = 38.86$ and 48.70° also appeared, due to the formation of monoclinic CuO (PDF # 65-2309). These observations indicate that in an acidic solution, WO_4^{2-} prefers to react with H^+ to produce H_2WO_4 , followed by partial and 70 complete dehydration to $\text{WO}_3 \cdot 0.33\text{H}_2\text{O}$ and WO_3 . In a basic solution, WO_4^{2-} turns to react with Cu^{2+} to produce $\text{Cu}_2\text{WO}_4(\text{OH})_2$ and $\text{CuWO}_4 \cdot 2\text{H}_2\text{O}$. In this case, $\text{Cu}(\text{OH})_2$ might be also formed, followed by dehydration to CuO .

After the above samples were sintered at 500 °C, there were 75 great changes in the crystal structures and phase composition (Fig. 1B). With the sample prepared at pH 1.1, the original phases of hexagonal WO_3 and $\text{WO}_3 \cdot 0.33\text{H}_2\text{O}$ completely disappeared, together with the formation of new phases of monoclinic WO_3 (PDF # 43-1035) and triclinic CuWO_4 (PDF # 21-0307). This 80 observation indicates that there is a solid-state reaction between tungstate and cupric species present in the un-sintered samples. As the synthesis pH increased, the phase contents of WO_3 and CuWO_4 decreased and increased, respectively. Moreover, with the sample prepared at pH 11.6, the diffraction peaks due to 85 crystalline CuO were also visible. Since the XRD technique has a certain detection limit, it follows that the phase contents of WO_3 and CuO in the mixtures decrease and increase with the synthesis pH, respectively.

The solid composition that changes with the synthesis pH is 90 also suggested by the diffuse reflectance spectra (Fig. 2). As the

synthesis pH increased, not only the spectral onset of the sample shifted gradually from 480 nm toward a longer wavelength,

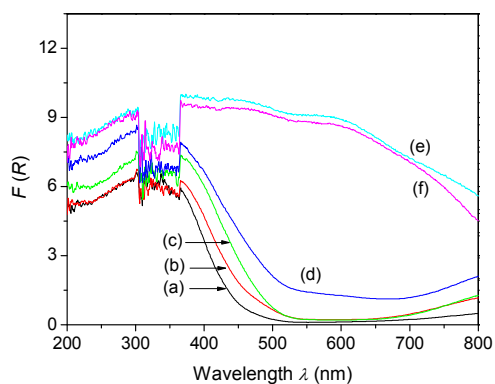


Fig. 2 Diffuse reflectance spectra of the powders sintered at 500 °C. Samples were hydrothermally synthesized at different pHs of (a) 1.1, (b) 2.4, (c) 3.9, (d) 5.2, (e) 8.5, and (f) 11.6, respectively.

but also the absorbance at given wavelength increased. In comparison, the spectral onset of pure WO_3 and CuWO_4 were located at 480 and 540 nm, respectively, while the absorption spectrum of black CuO expanded in the whole wavelength region (data not shown here). It becomes clear that increasing the synthesis pH leads to a gradual phase transition from WO_3 to CuWO_4 to CuO , the trend of which is in good agreement with that observed from XRD.

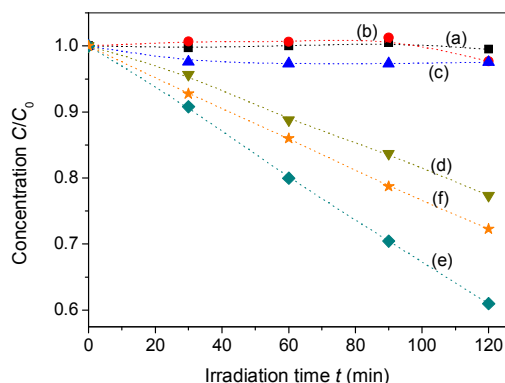


Fig. 3 Photocatalytic degradation of X3B under visible light in aerated aqueous suspensions. Catalysts were prepared at different pHs of (a) 1.1, (b) 2.4, (c) 3.9, (d) 5.2, (e) 8.5, and (f) 11.6, followed by sintering at 500 °C in air for 3 h.

Photocatalytic activity of the sintered sample was evaluated under visible light by using X3B degradation as a model reaction, and the result is shown in Fig. 3. This azo-dye was stable against photolysis. In the presence of catalyst, the concentration of X3B in solution decreased with the irradiation time, indicative of the dye degradation. However, different catalysts showed different activities. A maximum rate of X3B degradation was observed with the catalyst prepared at pH 8.5. On the other hand, these catalysts were also different in their sorption capacities toward X3B in water. The amount of X3B adsorption (q_e), measured in the dark, was negligible with the samples prepared at pH < 5.2, while the values of q_e with the samples prepared at pH 5.2, 8.5, and 11.6 were 1.0, 2.4 and 8.1 $\mu\text{mol/g}$, respectively. Since the trend in q_e among the catalysts does not match that in the rate of dye degradation, it can be concluded that W-rich and Cu-rich

CuWO_4 are less and more photoactive than CuWO_4 , respectively.

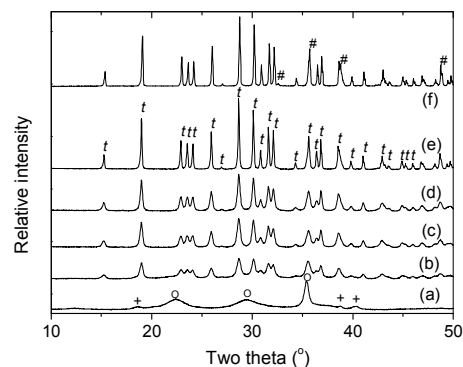


Fig. 4 XRD patterns of the sample prepared at pH 8.5, and sintered in air for 3 h at different temperatures of (a) 300, (b) 400, (c) 500, (d) 600, (e) 700, and (f) 800 °C. The captions are the same as those in Fig. 1.

Table 1. Physical parameters of Cu-rich CuWO_4 at different temperatures.

T_s (°C)	d_{XRD} (nm)	d_{SEM} (nm)	S_{BET} (m^2/g)	V_p (cm^3/g)
170	n.d	n.d	72.2	0.29
300	n.d	n.d	53.0	0.27
400	25.4	28.1	25.3	0.23
500	30.3	34.1	17.3	0.14
600	38.2	43.7	12.2	0.06
700	>100	406.4	0.10	n.d
800	>100	3260 × 940	n.d	n.d

^an.d., not detectable; d_{XRD} , crystallite size by XRD; d_{SEM} , particle size by SEM; S_{BET} , BET specific surface area; V_p , total pore volume.

Effect of Sintering Temperature

Since Cu-rich sample is superior to W-rich sample, a further study has been made with the Cu-rich CuWO_4 prepared at pH 8.5. Fig. 4 shows the XRD patterns of the samples sintered in air at different temperatures (T_s) for 3 h. At 300 °C, the sample was a mixture of $\text{CuWO}_4 \cdot 2\text{H}_2\text{O}$ and $\text{Cu}_2\text{WO}_4(\text{OH})_2$, similar to the unsintered sample (curve e, Fig. 2A). However, at 400 °C, these phases of $\text{CuWO}_4 \cdot 2\text{H}_2\text{O}$ and $\text{Cu}_2\text{WO}_4(\text{OH})_2$ completely disappeared, together with the formation of CuWO_4 . As T_s further increased, the diffraction intensity of CuWO_4 increased, indicative of the crystal growth. Moreover, at 800 °C, the crystalline phase of CuO was clearly observed. By using the Scherrer equation, the average crystallite size (d_{XRD}) of CuWO_4 for each sample was estimated, and the result is tabulated in Table 1. There is indeed a progressive increase in the primary crystallite size as T_s increases.

The surface area (S_{BET}) and pore volume (V_p) of the solid were measured by N_2 adsorption at 77 K. As T_s increased, both the values of S_{BET} and V_p decreased. Since N_2 largely adsorbs onto the solid external surface, it follows that the particle size of the whole mixture also increases with T_s . To distinguish the crystal and particle growth, the SEM images were recorded with all the samples (Fig. 5). At low T_s , the particles were highly aggregated and opaque in appearance. As T_s increased, the contour between the particles became more and more clear. At the same time, the average grain size was significantly increased, from 28.1 nm at 400 °C, to 406.4 nm at 700 °C (Table 1). At 800 °C, the rod-like particles were produced, with an average size of 3.26 μm in length and 0.94 μm in width. These observations suggest that the primary crystallites of CuWO_4 grow to big crystals on the thermal

treatment. Moreover, there were also some small particles on the

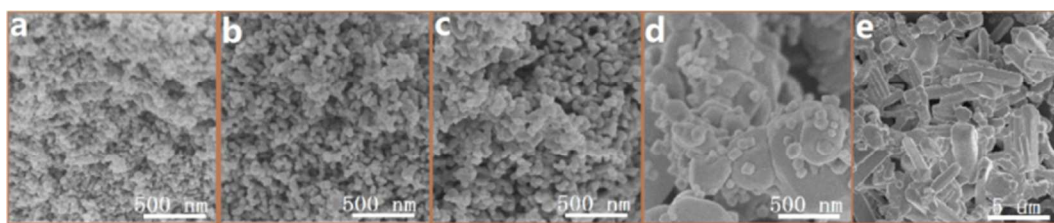


Fig. 5 SEM images of the sample prepared at pH 8.5, and sintered at (a) 400, (b) 500, (c) 600, (d) 700, and (e) 800 °C.

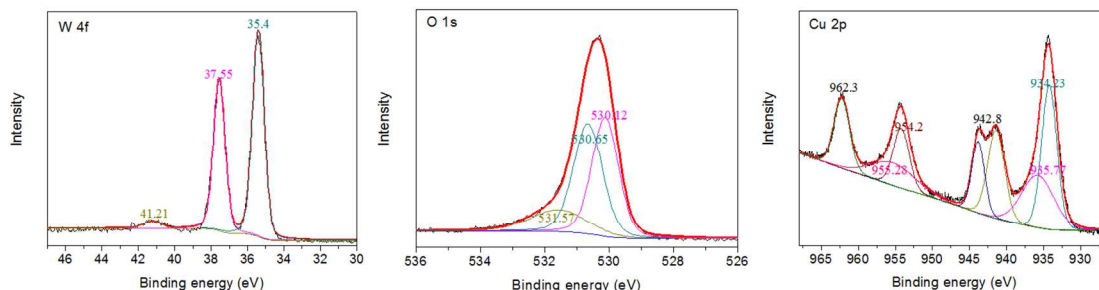


Fig. 6 X-ray photoelectron spectra of W(4f), O(1s) and Cu(2p) for the sample prepared at pH 8.5, and sintered at 600 °C for 3h. The colored curves correspond to deconvolution with a Lorentzian-Gaussian function.

large particles (Fig. 5d). According to the crystallite size of CuWO_4 , the observed small and large particles are presumably assigned to CuO , and CuWO_4 , respectively.

Fig. 6 shows the XPS spectra of W, O and Cu for the sample sintered at 600 °C. The binding energies of $\text{W}(4f_{7/2})$, $\text{W}(4f_{5/2})$ and $\text{W}(5p_{3/2})$ at 35.4, 37.6 and 41.2 eV were in good agreement with the standard data for W^{6+} .¹⁴ By using a Lorentzian-Gaussian function, the peak of $\text{O}(1s)$ at 530.4 eV were deconvoluted into three peaks: W-O (530.1 eV), Cu-O (530.6 eV), and surface OH^- (531.6 eV).^{15–18} The peaks of $\text{Cu}(2p_{3/2})$ and $\text{Cu}(2p_{1/2})$ at 934.3 and 954.3 eV could be also deconvoluted into two components: 934.2, and 935.8 eV for $\text{Cu}(2p_{3/2})$; 954.2, and 955.3 eV for $\text{Cu}(2p_{1/2})$. The binding energies of $\text{Cu}(2p_{3/2})$ at 934.2 eV and $\text{Cu}(2p_{1/2})$ at 954.2 eV were similar to those reported with CuO ,^{19–24} while the remaining peaks are due to Cu(II) in the lattice sites of CuWO_4 . In addition, there were two shakeup satellite peaks at 943 and 963 eV, typical of Cu(II) in cupric compounds.²⁵ These observations indicate that this sample is a mixture of CuWO_4 and CuO , and that only the chemical states of Cu(II) and W(VI) are present.

Fig. 7A shows the results of X3B degradation in aerated aqueous suspension under visible light. With each catalyst, the concentration of X3B in solution decreased with the irradiation time. Among the catalysts, the rates of dye degradation were different. A maximum rate of dye degradation was observed with the sample sintered at 400 °C. However, these catalysts had different values of q_e . Since the rate of dye degradation increase with its surface concentration, the observed rate should be normalized with q_e for evaluation of the catalyst activity. This specific rate reached a maximum with the catalyst sintered at 600 °C. However, X3B is red in color, and its degradation may occur through dye sensitization, other than photocatalytic pathway.²⁶ Because of that, it is better to use a colorless compound as a model substrate such as phenol. Fig. 7B shows the result of phenol degradation in water, measured under UV light for a fast data collection. Interestingly, the relative activity among the

catalysts observed from phenol degradation under UV light was

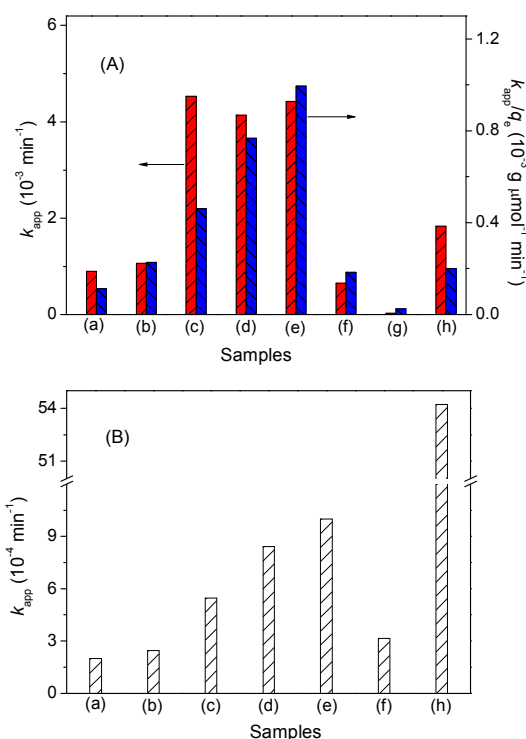
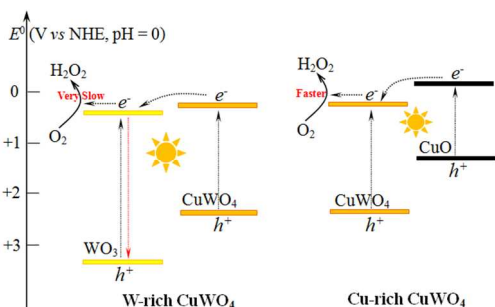


Fig. 7 (A) Rate constant (k_{obs}) and q_e -normalized k_{obs} for X3B degradation in aqueous solution under visible light. (B) Rate constant of phenol degradation in aqueous solution under UV light. The catalysts were prepared at pH 8.5, followed by sintering in air for 3 h at (a) 100, (b) 300, (c) 400, (d) 500, (e) 600, (f) 700, (g) 800 °C, and (h) commercial P25.

similar to that observed from dye degradation under visible light (Fig. 7A). A maximum activity was also obtained with the sample sintered at 600 °C. Such T_s -dependent activity observed with Cu -rich CuWO_4 is similar to those reported with other semiconductor photocatalysts.² With the increase of T_s , the increase of crystallinity (Fig. 5) and the decrease of surface area (Table 1)

would benefit and disbenefit the photocatalytic reaction, respectively. As a result, the optimum T_s of 600 °C is observed with the Cu-rich CuWO_4 (Fig. 7). As a reference, the commercial TiO_2 of Degussa P25 was also used as a photocatalyst. Under visible light, this TiO_2 was active for X3B degradation, due to the dye sensitization. But this activity of TiO_2 is much lower than that of the Cu-rich CuWO_4 sintered at 400–600 °C. Under UV light for phenol degradation, TiO_2 was always more active than that obtained with any of Cu-rich CuWO_4 samples.



Scheme 1. Band structures of WO_3 , CuO and CuWO_4 in aerated aqueous suspension and possible interfacial transfers between two semiconductors.

Possible mechanism

It has been reported that the conduction band edge potentials (E_{CB}) for CuO , CuWO_4 , and WO_3 in water at pH 0, are -0.03 , $+0.20$, and $+0.30$ V versus normal hydrogen electrode (NHE), respectively.^{13,27} All these values of E_{CB} are more positive than the one-electron reduction potential of O_2 (-0.05 V vs NHE). Then, in thermodynamics, the one-electron reduction of O_2 would be not allowed, and consequently organic degradation on these photocatalysts was inactive, as observed with WO_3 and CuO .^{13,28} However, in the aerated aqueous suspension of CuWO_4 , organic degradation could occur under UV or visible light.^{11–13} In this case, the photocatalytic generation of H_2O_2 is also observed, ascribed to the two-electron reduction of O_2 over the irradiated CuWO_4 .¹³

In thermodynamics, the electron transfer from CuWO_4 to WO_3 , and the electron transfer from CuO to CuWO_4 are both possible (Scheme 1). However, the transferred electron on WO_3 hardly reacts with O_2 to form HO_2 or H_2O_2 .^{28,29} This may explain the observation that W-rich CuWO_4 is less active than CuWO_4 for organic degradation in an aerated aqueous suspension (Fig. 3). On the contrary, the transferred electron on CuWO_4 can be captured by O_2 to form H_2O_2 . As a result, the efficiency of charge separation is improved, and the rate of organic degradation is enhanced. However, at a high Cu/W ratio of 3.0, Cu-rich CuWO_4 becomes to be less active. Since black CuO is nearly not active, the decreased activity of Cu-rich CuWO_4 is due to the decreased concentration of net CuWO_4 in the reactor, and due to the reduced number of photons reaching CuWO_4 , and/or both.

Conclusion

In this work, CuWO_4 has been synthesized in aqueous medium at 170 °C through a hydrothermal reaction between Cu^{2+} and WO_4^{2-} . However, due to the pH-dependent hydrolysis of precursors, this material is easily contaminated by WO_3 or CuO . The optimal pH for the synthesis of stoichiometric CuWO_4 is around 5.2. On the

other hand, these composite materials have different activities for organic degradation in aerated aqueous solution under UV and visible light. Comparatively, W-rich and Cu-rich CuWO_4 are less and more active than CuWO_4 , respectively. Furthermore, the photocatalytic activity of Cu-rich CuWO_4 is also a function of its sintering temperature, mainly ascribed to the combined effects of crystallinity and surface area. The present result would be useful to further development of the CuWO_4 -based photocatalysts for environmental use, and for water splitting as well.

Acknowledgements.

This work was supported by the 973 program of China (No. 2011CB936003) and NSFC (No. 21377110).

Notes and references

- State key Laboratory of Silicon Materials and Department of Chemistry, Zhejiang University, Hangzhou, 310027, China.
E-mail: xuyun@zju.edu.cn
- †Electronic Supplementary Information (ESI) available: [details of EDS spectra]. See DOI: 10.1039/b000000x/
- M. R. Hoffmann, S. T. Martin, W. Choi, D. W. Bahnemann, *Chem. Rev.* 1995, **95**, 69.
- O. Carp, C. L. Huisman, A. Reller, *Prog. Solid State Chem.* 2004, **32**, 33.
- T. L. Thompson, J. T. Yates, *Chem. Rev.* 2006, **106**, 4428.
- R. Lacomba-Perales, J. Ruiz-Fuertes, D. Errandonea, D. Martínez-García, A. Segura, *EPL*. 2008, **83**, 37002.
- J. E. Yourey, K. J. Pyper, J. B. Kurtz, B. M. Bartlett, *J. Phys. Chem. C* 2013, **117**, 8708.
- J. C. Hill, K. S. Choi, *J. Mater. Chem. A* 2013, **1**, 5006.
- J. E. Yourey, B. M. Bartlett, *J. Mater. Chem.* 2011, **21**, 7651.
- J. E. Yourey, J. B. Kurtz, B. M. Bartlett, *J. Phys. Chem. C* 2012, **116**, 3200.
- Y. Chang, A. Braun, A. Deangelis, J. Kaneshiro, N. Gaillard, *J. Phys. Chem. C* 2011, **115**, 25490.
- N. Gaillard, Y. Chang, A. DeAngelis, S. Higgins, A. Braun, *Inter. J. Hydrogen Energy* 2013, **38**, 3166.
- T. Montini, V. Gombac, A. Hameed, L. Felisari, G. Adami, P. Fornasiero, *Chem. Phys. Lett.* 2010, **498**, 113.
- U. M. García-Pérez, A. Martínez-de la Cruz, J. Peral, *Electrochim. Acta.* 2012, **81**, 227.
- H. Chen, Y. Xu, *J. Phys. Chem. C* 2014, **118**, 9982.
- S. Penner, X. Liu, B. Klotzer, F. Klauser, B. Jenewein, E. Bertel, *Thin. Solid. Films* 2008, **516**, 2829.
- J. H. Pan, W. I. Lee, *Chem. Mater.* 2006, **18**, 847.
- M. R. Bayati, F. Golestani-Fard, A. Moshfegh, Z. R. Molaei, *Mater. Chem. Phys.* 2011, **128**, 427.
- S. Poulston, P. M. Parlett, P. Stone, M. Bowker, *Surf. Interface Anal.* 1996, **24**, 811.
- M. Takeuchi, Y. Shimizu, H. Yamagawa, T. Nakamuro, M. Anpo, *Appl. Catal. B: Environ.* 2011, **110**, 1.
- G. Moretti, G. Fierro, M. L. Jacono, P. Porta, *Surf. Interface Anal.* 1989, **14**, 325.
- G. Deroubaix, P. Marcus, *Surf. Interface Anal.* 1992, **18**, 39.
- T. Robert, M. Bartel, G. Offergeld, *Surf. Sci.* 1972, **33**, 123.
- B. R. Strohmeier, D. E. Leyden, R. S. Field, D. M. Hercules, *J. Catal.* 1985, **94**, 514.
- F. Parmigiani, G. Pacchioni, F. Illas, P. S. Bagus, *J. Electron Spectrosc. Relat. Phenom.* 1992, **59**, 255.
- J. G. Jolley, G. G. Geesey, M. R. Hankins, R. B. Wright, P. L. Wichlacz, *Appl. Surf. Sci.* 1989, **37**, 469.
- T. L. Hsiung, H. P. Wang, Y. Lu, M. C. Hsiao, *Rediat. Phys. Chem.* 2006, **75**, 2054.
- K. Lv, Y. Xu, *J. Phys. Chem. B* 2006, **110**, 6204.
- J. R. Darwent, A. Mills, *J. Chem. Soc., Faraday Trans.* 1982, **78**, 359.

28 J. Kim, C. W. Lee, W. Choi, *Environ. Sci. Technol.* 2010, **44**, 6849.

29 J. Sheng, X. Li, Y. Xu, *ACS Catal.* 2014, **4**, 732.